



## Coupled oscillator models with no scale separation

Philip Du Toit<sup>a,\*</sup>, Igor Mezić<sup>b</sup>, Jerrold Marsden<sup>a</sup>

<sup>a</sup> Control and Dynamical Systems, California Institute of Technology, MC 107-81, Pasadena, CA 91125, United States

<sup>b</sup> Department of Mechanical Engineering, University of California Santa Barbara, Santa Barbara, CA 93106, United States

### ARTICLE INFO

#### Article history:

Received 23 June 2008

Received in revised form

9 October 2008

Accepted 19 November 2008

Available online 10 December 2008

Communicated by V. Rom-Kedar

#### PACS:

87.15.hp

87.15.hj

#### Keywords:

Coarse variables

Reduced model

Coupled oscillators

Dynamics of biomolecules

### ABSTRACT

We consider a class of spatially discrete wave equations that describe the motion of a system of linearly coupled oscillators perturbed by a nonlinear potential. We show that the dynamical behavior of this system cannot be understood by considering the slowest modes only: there is an “inverse cascade” in which the effects of changes in small scales are felt by the largest scales and the mean-field closure does not work. Despite this, a one and a half degree of freedom model is derived that includes the influence of the small-scale dynamics and predicts global conformational changes accurately. Thus, we provide a reduced model for a system in which there is no separation of scales. We analyze a specific coupled-oscillator system that models global conformation change in biomolecules, introduced in [I. Mezić, On the dynamics of molecular conformation, Proc. Natl. Acad. Sci. 103 (20) (2006) 7542–7547]. In this model, the conformational states are stable to random perturbations, yet global conformation change can be quickly and robustly induced by the action of a targeted control. We study the efficiency of small-scale perturbations on conformational change and show that “zipper” traveling wave perturbations provide an efficient means for inducing such change. A visualization method for the transport barriers in the reduced model yields insight into the mechanism by which the conformation change occurs.

© 2008 Elsevier B.V. All rights reserved.

## 1. Introduction

Averaging over fast variables is a widely used method to obtain coarse equations of motion in mechanical systems with many degrees of freedom [1]. For example, averaging methods have been successfully used to find accurate coarse models in celestial mechanics and in oscillating electrical circuits. In this paper, however, we study a system of nonlinearly perturbed coupled oscillators that exhibits resonances on all scales and consequently does not admit analysis using standard averaging techniques. Furthermore, the full system, as will be demonstrated using a simple bio-mechanical example, has interesting dynamics that includes spontaneous and coherent changes in global conformation, and reduction of the system using straightforward truncation methods fails to capture the crucial influence of the fine-scale dynamics that induces this conformation change.

The class of nonlinear systems of coupled oscillators that we study are close to a coupled chain of linear harmonic oscillators. Such near-integrable systems have been studied in [2] where transition to equipartition of energy and dynamical properties related to integrable instability theory of partial differential equations were investigated [3]. Here we discuss the representation of dynamics of the full oscillator system as a  $1\frac{1}{2}$

degree of freedom oscillator that provides a good representation of certain aspects of the full dynamics such as coherent switching between equilibria described in a biomechanical example of [4] that builds on the models for DNA dynamics described in [5].

We begin by presenting an approximation to the full coupled oscillator system that allows for the derivation of a single coarse equation that retains essential contributions from the higher order components. Moreover, the resulting single degree of freedom system faithfully captures the statistics of the interesting conformation change behavior observed in the full system. The approximation involves, in essence, replacing higher order components in the perturbed problem with corresponding analytic trajectories for the nearby linear system.

For the bio-mechanical example system, we also investigate robust actuation of conformation change and demonstrate that low-powered traveling wave perturbations provide an efficient means for achieving near optimal conformation change. A method for visualizing transport structures will be introduced and applied to the dynamics describing the coarse variables, and consequently lend insight into the transport mechanisms that allow for the global conformation change to occur.

## 2. Coarse variables and models

Consider the following system of ordinary differential equations:

$$\ddot{\theta}(t) + D \cdot \theta(t) = \epsilon F(\theta(t), t) \quad (1)$$

\* Corresponding author. Tel.: +1 626 395 4882; fax: +1 626 3956170.  
E-mail address: [pdutoit@cds.caltech.edu](mailto:pdutoit@cds.caltech.edu) (P. Du Toit).

with initial conditions

$$\theta(0) = a \quad \dot{\theta}(0) = b$$

where  $a, b$ , and  $\theta(t)$  are vectors in  $\mathbb{R}^N$  ( $\dot{\theta}$  and  $\ddot{\theta}$  denote the first and second derivative of the components of  $\theta$  with respect to the independent variable  $t$  respectively),  $F : \mathbb{R}^N \times \mathbb{R} \rightarrow \mathbb{R}^N$  is a nonlinear time-dependent mapping,  $\epsilon > 0$  is a small parameter that controls the size of the nonlinear perturbation, and  $D : \mathbb{R}^N \rightarrow \mathbb{R}^N$  is a linear mapping that has the tri-diagonal matrix representation

$$D = \begin{bmatrix} 2 & -1 & 0 & & & 0 & -1 \\ -1 & 2 & -1 & 0 & & & 0 \\ 0 & -1 & 2 & -1 & 0 & & \\ & \ddots & \ddots & \ddots & \ddots & \ddots & \\ & & 0 & -1 & 2 & -1 & 0 \\ 0 & & & 0 & -1 & 2 & -1 \\ -1 & 0 & & & 0 & -1 & 2 \end{bmatrix}$$

The smoothness conditions we require are that  $F(\theta, t)$  is continuous in  $t$  and Lipschitz-continuous in  $\theta$ . Equation (1) and the initial conditions can be written in component form using subscripts to denote the indices as

$$\begin{aligned} \ddot{\theta}_k &= \theta_{k+1} - 2\theta_k + \theta_{k-1} + \epsilon F_k(\theta, t) & k = 1, \dots, N \\ \theta_k(0) &= a_k & \dot{\theta}_k(0) = b_k \end{aligned}$$

where  $\theta_0 = \theta_N$  defines the periodic boundary condition.

Such a system arises naturally from a spatial discretization of a nonlinearly perturbed wave equation with periodic boundary conditions

$$u_{tt}(x, t) = u_{xx}(x, t) + \epsilon G(x, u(x, t), t)$$

where  $u : \mathbb{R} \times \mathbb{R} \rightarrow \mathbb{R}$  is the amplitude of the wave in time and space (subscripts denote partial differentiation), and the real-valued function  $G$  represents the perturbation. In this context, the  $D$  matrix in Eq. (1) is simply a centered finite differencing operator that approximates the second partial derivative of  $u$  with respect to the spatial variable  $x$ , and  $F$  is obtained by evaluating  $G$  at uniformly discrete spatial positions  $x_k$  so that  $F_k(\theta, t) := G(x_k, \theta, t)$ ,  $\theta_k(t) := u(x_k, t)$ , and  $x_0 = x_N$ .

Equivalently, Eq. (1) can be viewed as the dynamical system describing a linear chain of  $N$  oscillators in which each oscillator is subject to a weak nonlinear potential and coupled to nearest neighbors through a harmonic potential; a specific example of such an oscillator chain related to the mechanics of biomolecules will be provided later. E. Fermi, J. Pasta, S. Ulam, and M. Tsingou used a similar chain of coupled oscillators as an example system in their pioneering numerical study of nonlinear dynamics that has since become famously known as the Fermi–Pasta–Ulam–Tsingou<sup>1</sup> (FPUT) problem [7]. The initial purpose of their study was to develop a theory of thermalization in systems with nonlinear dynamics. However, their investigation yielded unexpected results – energy initially placed in one mode did not become equally partitioned among all the modes after some time. Rather, they observed recurrences where the energy initially redistributed among some of the modes but then returned to the initial condition in which all the energy is again found in a single mode. Analyses of the FPUT problem fill a large body of literature including, for instance, the discovery of soliton and chaotic breather solutions,

<sup>1</sup> Historically, this problem has been referred to as the Fermi–Pasta–Ulam (FPU) problem, however, recently the contribution of Mary Tsingou to the implementation of the numerical routines has been more widely appreciated, motivating the addition of her name. The recent article in [6] provides a discussion of the relevant history.

and have yielded insight into the interplay between chaos and integrability in nonlinear systems (see Ref. [8] for a survey of results related to the FPUT problem on the fiftieth anniversary of the introduction of the problem). The approach to the problem addressed in this paper differs from traditional FPUT problem analyses in that, motivated by the biomolecular applications to DNA, we are interested in issues such as reduction to coarse variables and activation of global large-scale conformation change through the application of small local controls that are not typically associated with the FPUT problem.

We study the system of ordinary differential equations described by Eq. (1) when  $N$  is large and hence the system has many degrees of freedom. Rather than determine precisely the dynamics of each degree of freedom, we are interested in describing the dynamics of only a single coarse variable. The first question to be addressed here is the following: how do we extract from the large  $N$  degree of freedom system an evolution equation for a single coarse variable that describes a property of interest. For the purposes of the current study, our goal is to determine a single evolution equation for the dynamics of the *average* amplitude while faithfully retaining salient dynamical features of the full system. As will be shown later, the dynamics of the coarse variable will need to include the influence of the fine scales in order to reproduce the coarse evolution correctly. We begin by first gaining insight from the unperturbed case.

### 2.1. The unperturbed case

When  $\epsilon = 0$ , the system in Eq. (1) becomes:

$$\ddot{\theta}(t) + D \cdot \theta(t) = 0 \tag{2}$$

with initial conditions

$$\theta(0) = a \quad \dot{\theta}(0) = b.$$

This is a simple linear system whose solution is easily obtained analytically. The solution is provided here in detail, as it includes many building blocks required for the less tractable case when the nonlinear perturbation is included.

We begin by introducing a change of coordinates that diagonalizes the coupling matrix  $D$ . Let  $P$  be an  $N \times N$  matrix whose columns contain the complete set of orthonormal eigenvectors of the real symmetric matrix  $D$ :

$$P_{kw} := \sqrt{\frac{2}{N}} \begin{bmatrix} \frac{1}{\sqrt{2}} & \cos \frac{2\pi kw}{N} & \frac{(-1)^k}{\sqrt{2}} & \sin \frac{2\pi kw}{N} & \vdots \\ w=0 & w=[1 \dots \frac{N}{2}-1] & w=\frac{N}{2} & w=[\frac{N}{2}+1 \dots N-1] & \vdots \end{bmatrix} \tag{3}$$

(Here we have taken  $N$  to be even, for simplicity, although the case for odd  $N$  merely has the middle column corresponding to  $w = \frac{N}{2}$  removed and the column numbering altered accordingly.)

Next, we define new coordinates by the linear transformation

$$\hat{\theta} := P' \theta \tag{3}$$

where  $P'$  denotes the transpose of  $P$ . Notice that

$$\hat{\theta}_0 := \frac{1}{\sqrt{N}} \sum_{k=1}^N \theta_k \tag{4}$$

is (except for a constant factor of  $\sqrt{N}$ ) the average amplitude. In these coordinates, the symmetric linear operator  $D$  is diagonal,

yielding  $N$  uncoupled second order ODEs. In component form, they are written as

$$\ddot{\theta}_0 = 0 \tag{5a}$$

$$\ddot{\theta}_w + \alpha_w^2 \hat{\theta}_w = 0 \quad w = 1, \dots, N - 1 \tag{5b}$$

where  $\alpha_w^2 := 2 \left(1 - \cos \frac{2\pi w}{N}\right)$ , and the initial conditions become

$$\hat{\theta}(0) = P'a =: \hat{a} \quad \dot{\hat{\theta}}(0) = P'b =: \hat{b}.$$

Here we can immediately conclude that the evolution of the average amplitude in the unperturbed case is given by the single scalar equation

$$\hat{\theta}_0(t) = \hat{a}_0 + \hat{b}_0 t.$$

Straightforward solution of the higher order components yields the analytic evolution equations

$$\hat{\theta}_w(t) = \hat{a}_w \cos \alpha_w t + \frac{\hat{b}_w}{\alpha_w} \sin \alpha_w t \quad w = 1, \dots, N - 1. \tag{6}$$

We readily observe that the system has  $N$  integrals of motion,  $\{I_w\}_{w=0}^{N-1}$ , defined by

$$\begin{aligned} \dot{\hat{\theta}}_0(t) &= (\hat{b}_0) =: \sqrt{2I_0} \\ \hat{\theta}_w(t)^2 + \left(\frac{\dot{\hat{\theta}}_w(t)}{\alpha_w}\right)^2 &= (\hat{a}_w)^2 + \left(\frac{\hat{b}_w}{\alpha_w}\right)^2 =: 2I_w \\ w &= 1, \dots, N - 1. \end{aligned}$$

The first integral is simply a statement of the conservation of total (or average) momentum. The higher order modes evolve on circles of constant radii  $\sqrt{2I_w}$  with an angular frequency of  $\alpha_w$ . With these insights, we may write the system in completely integrable Hamiltonian form using action angle coordinates  $(I, \phi)$  where  $I$  and  $\phi$  are both vectors of length  $N$  whose components  $I_w$  and  $\phi_w$  are denoted with subscripts:

$$H^0(I_0, \dots, I_{N-1}) = \sum_{w=1}^{N-1} \alpha_w I_w \tag{7}$$

so that the Hamiltonian vector field becomes

$$\begin{aligned} \dot{I}_w &= -\frac{\partial H^0}{\partial \phi_w}(I_0, \dots, I_{N-1}) = 0 \\ \dot{\phi}_w &= \frac{\partial H^0}{\partial I_w}(I_0, \dots, I_{N-1}) = \alpha_w \quad w = 0, \dots, N - 1. \end{aligned}$$

Before proceeding to an analysis of the perturbed case, we first observe here some of the important properties of the unperturbed system.

**Remark.** The Hamiltonian  $H^0$  is degenerate.

The Hamiltonian  $H^0$  is linear in the components of  $I$ ; hence

$$\det \left( \frac{\partial^2 H^0}{\partial I_i \partial I_j}(I_0, \dots, I_{N-1}) \right) = 0 \quad i, j = 0, \dots, N - 1, \tag{8}$$

and the frequency map  $I \rightarrow \alpha(I)$  is not a diffeomorphism. This degeneracy of the Hamiltonian implies that the system does not satisfy the assumptions of classical KAM theorems, and hence straightforward KAM theory cannot be applied [9]. For the FPUT system, a version of the KAM theorem has been proven in [10]; however, in this paper we do not need or use a KAM result.

**Remark.** The frequency vector  $\alpha$  is resonant.

Since the first element of the frequency vector  $\alpha$  is 0, any  $\kappa \in \mathbb{Z}^N \setminus \{0\}$  of the form  $\kappa = [z \ 0 \ \dots \ 0]'$  for any  $z \in \mathbb{Z} \setminus \{0\}$  yields  $\kappa \cdot \alpha = 0$ . The irrational structure of the eigenvalues in the higher modes leads to the conclusion that the resonant frequency vector  $\alpha$  is of multiplicity 1. Furthermore, since  $z$  is any element in  $\mathbb{Z} \setminus \{0\}$ , we can conclude the following:

**Remark.** The frequency vector  $\alpha$  has resonances at all orders.

A standard approach to achieve reduction of order in a dynamical system is to perform averaging over the fast angular coordinates. However, for the system of interest, the resonances, or more specifically the zero eigenvalue corresponding to  $\alpha_0 = 0$  in the equation for the average amplitude, precludes such a treatment. Standard statements of averaging theorems require all the components of the frequency vector  $\alpha$  to be strictly greater than 0 (see the statement of the Averaging Theorem in [11], for example, or the discussion in chapter 8 of [1] regarding passage through resonance and the absence of theory to treat the fully resonant case). Hence, the oscillator system represents a special case to which routine averaging methods cannot be applied.

Moreover, in our attempt to obtain a single closed equation for the evolution of the average variable, straightforward averaging or truncation approaches are ineffective for an even more subtle—yet crucial—reason. Averaging over the the higher order components (laying the resonance issues aside) yields a single degree of freedom and hence integrable system. As such, the reduced equation fails to capture important details in the dynamics arising from the inherent non-integrability, and in particular the intricate influence of the higher order components on the average mode. A thorough review of averaging methods is not within the scope or purpose of this paper. However, an important point to be made is that a central feature of the proposed method is that it incorporates in an approximate yet effective way the influence of the higher order modes, and consequently more accurately captures nontrivial dynamics associated with the full non-integrable system. A partial averaging approach, as pursued in [12], is, however, capable of predicting aspects of the behavior, such as the energy of activation required for conformational change in biomechanical models described below.

### 2.2. Perturbed case

We use the same definitions and process used in the unperturbed case for the perturbed case. We begin by making the same linear change of coordinates using the matrix of eigenvectors  $P$  so that the transformed equations of motion become:

$$\ddot{\hat{\theta}}_0 = \epsilon P_{k0} F_k(P\hat{\theta}) \tag{9a}$$

$$\ddot{\hat{\theta}}_w + \alpha_w^2 \hat{\theta}_w = \epsilon P_{kw} F_k(P\hat{\theta}), \quad w = 1, \dots, N - 1, \tag{9b}$$

where we sum over  $k$  from 1 to  $N$  on the right hand side.

As expected, the coordinate transformation diagonalizes the nearest neighbor coupling term but the nonlinear forcing term remains globally coupled. At this stage, no approximations have been made and Eqs. (9a) and (9b) recover the full solution exactly. For nonzero  $\epsilon$ , the system is no longer integrable and the solutions that were previously observed to evolve on circles of fixed radii are perturbed.

At this point we must consider how to break the coupling between the zeroth order equation for the average amplitude and the higher order modes in order to obtain a closed equation for the average amplitude. As previously mentioned, the system is not amenable to averaging methods because of the zero eigenvalue in the frequency vector. Rather, we introduce an approximation by replacing Eq. (9b) with the analytical solutions of

the unperturbed linear system, as defined in Eq. (6). This approach effectively removes the need to integrate the higher order modes by replacing their evolution with the explicit analytic solution of the nearby integrable system. In so doing, we obtain the improved approximation,  $\bar{\theta}_0$ , of the exact solution  $\hat{\theta}_0$ , whose dynamics are prescribed by

$$\ddot{\bar{\theta}}_0 = \frac{\epsilon}{\sqrt{N}} \sum_{k=1}^N F_k(P\bar{\theta}) \quad (10)$$

where in the right hand side  $P$  is a constant matrix, and  $\bar{\theta}$  is a vector whose first component is the scalar dependent variable  $\bar{\theta}_0$  and whose remaining components are elementary functions of time and the initial conditions of the full system provided analytically by Eq. (6).

**Remark.** The solution trajectories of Eq. (10) are within  $\mathcal{O}(\epsilon)$  of the solution trajectories of the original full system described in Eq. (9a) for times  $\mathcal{O}(1)$ .

This result is shown by applying a standard error analysis technique: substituting a formal expansion of the solution, using the Lipschitz continuity of  $F$ , and then applying the Gronwall lemma as is done in the proof of Theorem 9.1 in [13] for example.

The approach proposed here for obtaining a closed equation for the average amplitude includes the influence of higher order modes by incorporating explicit time-dependence in the perturbing term, and hence leads to a one and a half degree of freedom system. The coordinate transformation and subsequent approximation yields a single *non-autonomous* ordinary differential equation that includes approximate dynamics for the higher order scales and whose solution approximates the dynamics of the average angle of the system. In effect, the information contained in the higher order modes persists in the lower order description via the initial conditions.

The method just described is now applied to a simple coupled-oscillator model for biomolecules, where retention of the influence of the higher modes in the dynamics is essential for accurately recovering nontrivial dynamics of conformation change.

### 3. Conformation change in biomolecules

Biomolecules undergo rapid and global conformation change as a crucial part of their function. Many statistical mechanical models have been proposed in which these conformation changes are the result of increased thermal fluctuations [14,5,15–18], or an external agent that provides an overwhelming force [19, 20]. Presently, we are interested in investigating whether this conformation change phenomenon can be induced simply by utilizing the natural dynamics inherent in the system. In [4] a simple model was presented in which the intrinsic design of the dynamics ensures the robustness of conformational states to random perturbations, yet global conformation change can be robustly induced by the action of a low-energy local control. At the heart of this dynamical behavior is the exchange of energy between smaller and larger scales. The approximation technique presented in the first section allows passage to a low-dimensional model that effectively captures this behavior.

#### 3.1. The model

We consider a class of biopolymers that can be modeled as a long circular chain of identical pendula attached to a rigid backbone. Each pendulum has one rotational degree of freedom in the plane orthogonal to the backbone. The motion of the pendula is governed by two interactions: each pendulum interacts

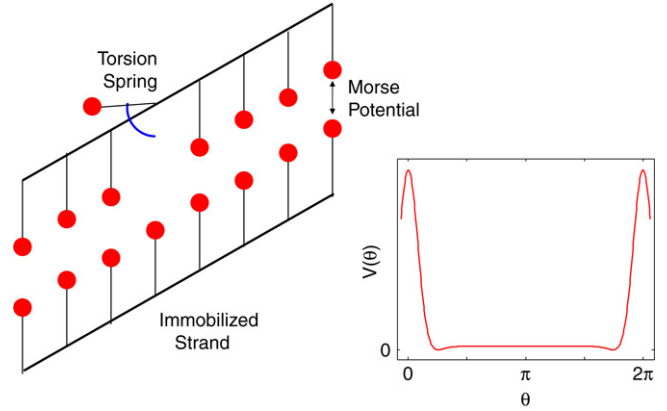


**Fig. 1.** The biomolecule is modelled as a chain of pendula that rotate about the axis of a fixed backbone. The pendula interact with nearest neighbors along the backbone through harmonic torsional coupling, and with pendula on the opposing strand through a Morse potential.

with its nearest neighbors through a harmonic potential that models torsional coupling through the backbone; and secondly, each pendulum moves in a Morse potential that models the weaker hydrogen bonding interaction between pendulum pairs on a complementary chain. We immobilize one of the strands and consider only the motion of the pendula on the opposing strand, as depicted in Fig. 1.

Using the pendulum mass,  $m$ , for the mass scale; the pendulum length,  $h$ , for the length scale; and the nearest neighbor coupling strength,  $S$ , for the energy scale; the non-dimensional Lagrangian that describes the motion of  $N$  coupled pendula is given by

$$L(\theta, \dot{\theta}) = \sum_{k=1}^N \left[ \frac{1}{2} \dot{\theta}_k^2 - \frac{1}{2} (\theta_k - \theta_{k-1})^2 - \epsilon \left( e^{-a[1-\cos \theta_k - x_0]} - 1 \right)^2 \right]$$

where  $a$ ,  $x_0$ , and  $\epsilon$  are the Morse potential decay coefficient, the Morse potential equilibrium distance, and the Morse potential amplitude, respectively. The angular displacement of the  $k$ th pendulum is denoted  $\theta_k$ . The argument of the Morse potential is the distance between complementary base pairs projected onto the vertical. The time,  $t$ , has been scaled by the induced non-dimensional time,  $\tau = \sqrt{S/(mh^2)}$ .

Lagrange's equations of motion yield

$$\ddot{\theta}_k - \theta_{k+1} + 2\theta_k - \theta_{k-1} = 2\epsilon a \left( e^{-a[1-\cos \theta_k - x_0]} - 1 \right) \times e^{-a[1-\cos \theta_k - x_0]} \sin \theta_k$$

for  $k = 1, \dots, N$ . These equations can also be written in the form introduced in Eq. (1):  $\ddot{\theta} + D \cdot \theta = \epsilon F(\theta)$  where  $D$  is the constant tridiagonal  $N \times N$  matrix that describes the nearest neighbor coupling, and  $F$  is the nonlinear vector-valued forcing term due to the Morse potential.

Numerical integration of the full system of equations was performed for a chain of  $N = 200$  pendula using a fourth order symplectic integrator with excellent energy preservation properties [21]. The parameter values were chosen to best represent typical values for biomolecules. The nondimensional scales are determined using parameter values  $m = 300$  AMU,  $h = 1$  nm, and  $S = 42$  eV, that collectively induce a model time unit of 0.272 ps. In nondimensional units the Morse potential parameters are  $a = 7$ ,  $x_0 = 0.3$ , and  $\epsilon = 1/1400$ . For these parameter values, the nonlinear Morse potential term represents a small perturbation to the linear nearest neighbor coupling interaction. A typical integration time over which we perform simulations is 300 units.

**Fig. 2.** Figure (a) shows sample phase space trajectories of a single pendulum in the Morse potential when no coupling is present. The homoclinic trajectory is emphasized. The locations of the equilibrium points are marked with red dots. Trajectories inside the homoclinic trajectory associated with the equilibrium point at  $(\pi, 0)$  are always oscillating, while those outside the homoclinic trajectory are always flipping. Figure (b) shows a single trajectory of the fully-coupled model projected onto the average variable phase space, and indicates a flipping event from one conformational state to the other. The trajectory resembles the phase portrait for a single pendulum moving in the Morse potential. However, the harmonic nearest neighbor coupling provides resonant kicks that allow the trajectory to escape from one energy basin and then become trapped by the other.

### 3.2. Properties of the model

The shape of the Morse potential induces two stable equilibria corresponding to global energy minima, achieved when all the pendula have identical angular displacements (thus nullifying the nearest neighbor coupling) and are positioned at the Morse potential equilibrium distance,  $x_0$ , from their complementary pendula. For small energies, typical motions involve uncoordinated oscillations of the pendula near these stable equilibria. It was observed in [4] that a local perturbation can cause the pendula to undergo a coherent global change of conformation from one energy basin to the other. By definition, we say that a global conformation change has occurred when the average angle of the pendula passes through  $\pi$  radians. This motion is referred to in the rest of this paper as “flipping”. A convenient way to represent this flipping behavior is to project the trajectory of the system onto the average variables  $\Theta := \frac{1}{N} \sum_{k=1}^N \theta_k$  and  $\dot{\Theta}$  as shown in Fig. 2(b). In this projection we see that the pendula at first oscillate about an energy minimum in one conformational state and then undergo conformational change to the other energy basin where they continue to oscillate.

### 3.3. The reduced order model

As noted above, the average angle variables provide a good coarse description of the flipping process and begs the derivation of a single closed equation for the average variable. There is, however, no separation of time scales in this system so that simple truncation to a low order model does not retain sufficient dynamics to incorporate spontaneous flipping events. Indeed, any method that yields an autonomous single degree of freedom system for the coarse variable, cannot possibly capture the flipping event. Furthermore, as we previously noted, routine averaging methods are not applicable, since intrinsic resonances induce coupling on all scales.

The approach presented in the first section is now applied to this pendulum chain to obtain a low order model that retains the essential influence of the higher order scales on the global flipping behavior. With no Morse potential ( $\epsilon = 0$ ), the remaining linear system has an explicit solution in which the average velocity  $\dot{\hat{\theta}}_0$  is constant, and the remaining coordinate pairs  $(\hat{\theta}_w, \dot{\hat{\theta}}_w)$  (after scaling  $\dot{\hat{\theta}}_w$  by its corresponding frequency  $\alpha_w$ ) evolve on circles of fixed radii. For small nonzero  $\epsilon$ , this integrable solution is

perturbed as shown in Fig. 3. Certainly, deviations from the linear solution are evident in the lower modes, whereas the trajectories of the higher order components remain close to the integrable circular solutions of the unperturbed case. Numerical experiments reveal that as epsilon is increased, the higher order components in a typical flipping trajectory remain close to the unperturbed solution until epsilon has increased by a factor of 10. As epsilon increases further, the higher order components still exhibit oscillatory behavior, but the stronger nonlinear coupling causes large deviations from the trajectories along fixed radii and the circular solutions disintegrate.

The  $1\frac{1}{2}$  degree of freedom reduced system obtained using the approximation in Eq. (10) retains sufficient dynamics of the higher order modes in the time-dependent terms to capture statistics of the the flipping event remarkably well. The distributions of numerically computed flipping times for 5000 random initial conditions for the  $1\frac{1}{2}$  degree of freedom reduced system and the full 200 degree of freedom system are compared in Fig. 4. The histograms in Figs. 4(a), (b), (c) are computed using values of epsilon equal to 1/1400, 5/1400, and 10/1400 respectively. When epsilon is equal to 1/1400 (the value provided by the biomolecule model), the reduced model captures the shape of the flipping time distribution remarkably well and the mean relative error in the predicted flipping time is less than five percent. As expected, the relative error in the flipping time prediction increases as epsilon is increased. The quasi-periodic forcing introduced in the right hand side of Eq. (10) by the solution for the linear system provides the perturbation required to induce global flipping from a local perturbation, and can be thought of as a time-dependent control.

The rigorous error estimate obtained in Section 2.2 stated that trajectories of the reduced model are within  $\mathcal{O}(\epsilon)$  of the true solution for times  $\mathcal{O}(1)$ . The application of this error estimate to the biomolecule model merits the following two observations. First, the portion of a trajectory during which the pendulum experiences the Morse potential (which is responsible for inducing flipping motion) is very brief; the interaction occurs on a time-scale that is  $\mathcal{O}(1)$  rather than the much longer  $\mathcal{O}(1/\epsilon)$  time-scale, so that the estimate has validity, as evidenced numerically, for the prediction of flipping times. Second, the error estimate was obtained for an arbitrary forcing function  $F(\theta(t), t)$ . In the biomolecule model, the exponential decay of the Morse potential with distance implies that when the pendula escape the immediate vicinity of the opposing pendula, the Morse potential and the consequent perturbation are effectively zero and the linear solution becomes nearly exact. Hence, the error estimate is conservative in that













